Journal of Molecular Liquids 218 (2016) 384–392

Contents lists available at ScienceDirect

Journal of Molecular Liquids

journal homepage: www.elsevier.com/locate/molliq

Experimental and quantum chemical studies on corrosion inhibition effect of 5,5 diphenyl 2-thiohydantoin on mild steel in HCl solution

Ayşe Ongun Yüce [a,*], Esra Telli [b], Başak Doğru Mert [a], Gülfeza Kardaş [a], Birgül Yazıcı [a]

[a] Çukurova University, Science and Letters Faculty, Chemistry Department, 01330 Adana, Turkey
[b] Osmaniye Korkut Ata University, Engineering Faculty, Energy Systems Engineering Department, 80000 Osmaniye, Turkey

ARTICLE INFO

Article history:
Received 16 November 2015
Received in revised form 31 December 2015
Accepted 26 February 2016
Available online xxxx

Keywords:
Corrosion inhibitor
Adsorption
Inhibition mechanism
Potential of zero charge

ABSTRACT

The inhibition efficiency of 5,5 diphenyl 2-thiohydantoin (DPTH) against mild steel (MS) corrosion has been investigated in 0.1 M HCl solution by using electrochemical techniques and quantum chemical calculations. The electrochemical measurements indicate that the inhibition efficiencies increase with the increasing concentration of DPTH. According to polarization measurements DPTH retards both anodic and cathodic reactions. Thermodynamic parameters and activation energy (E_a) for the MS corrosion have been determined from electrochemical results and discussed. Furthermore, quantum chemical parameters of DPTH have been calculated to explain the corrosion inhibition mechanism.

1. Introduction

Carbon steel is widely used as a preferential material for the metallurgical industries because of economical considerations. The disadvantage of these materials is being prone to corrosion when they are exposed to aggressive environments such as acids, bases and salts [1,2]. Among these environments, the acidic solutions in most industrial processes are commonly used for pickling, industrial acid cleaning, and acid descaling [3–6]. Unfortunately, iron and its alloys can be corroded during these acidic applications, particularly with the use of hydrochloric acid and sulfuric acid [7,8]. Hence, the prevention against corrosion of metals used in industrial applications is important to avoid the loss of resources and money [9–11]. Several initiatives are made to prevent the devastating effect of corrosion on metals and alloys in acid solutions. Corrosion control can be provided with the use of corrosion inhibitors, which is one of the most effective methods [12]. Most corrosion inhibitors are organic or inorganic chemicals reducing the deterioration of metals when added in small quantities to the corrosive environment. Among them, heterocyclic organic compounds containing sulfur, phosphorus, oxygen, nitrogen, electronegative functional groups and p-electron in triple or conjugated double bonds and aromatic rings are the most effective and efficient inhibitors for the metals in the acidic mediums due to their molecular structure [13–15]. The adsorption of organic compounds mainly depends on its physicochemical properties such as its electronic structure functional groups, steric effects, p-orbital character of donating electrons and electronic density of donor atoms [16]. The adsorption occurs due to the interaction of the lone pair and/or p-orbital of the inhibitor with d-orbital of the metal surface atoms resulting in the formation of a barrier film [17].

Thiohydantoin is sulfur analogs of hydantoins, which was formed with one or both carbonyl groups replaced by thiocarbonyl groups [18]. Among the known thiohydantoins, 2-thiohydantoins were used as the corrosion inhibitors [19] as well as the development of metal cation complexation and polymerization catalysis [20]. Furthermore, DPTH which is 2-thiohydantoin derivative was used as antioxidants [21] and in cancer research [22].

DPTH molecule contains sulfur, oxygen, two nitrogen atoms and phenyl groups. In the present study, the choice of DPTH is based on the presence of electron clouds on the aromatic rings and electronegative nitrogen and sulfur, oxygen atoms inducing greater adsorption of the compound on the MS surface.

Our study aims to investigate the efficiency of DPTH as the corrosion inhibitors in the hydrochloric acid mediums by using electrochemical techniques and quantum modeling.

2. Experimental

2.1. Preparation of electrodes

The working electrode was a cylindrical rod having a certain chemical composition cut from MS bar (wt); 0.17 C, 0.59 Si, 1.60 Mn, 0.04 P and Fe (remainder). The metal rod's surface area except a portion of 0.50 cm^2 was covered with polyester in order to work with a constant surface area during all measurements. Prior to each application, the surface of the working electrode was ended with the 1200 type after

* Corresponding author.
E-mail address: ayseongunyuce@gmail.com (A.O. Yüce).

http://dx.doi.org/10.1016/j.molliq.2016.02.087
0167-7322/

mechanically abraded by using different types of sand papers. The metal rod was dried with a filter paper after it was washed with bidistilled water, ethanol, and bidistilled water, respectively. The same application was repeated for each experiment.

2.2. Test solutions

The test solution is chosen as a 0.1 M $HCl_{(aq)}$ which is the most-used acid for degreasing, descaling, pickling, etc. The applications were carried out in 0.1 M HCl solution in the absence and in the presence of various concentrations (0.005 mM; 0.01 mM; 0.05 mM; 0.1 mM) of DPTH given chemical structure in Fig. 1. DPTH and other chemicals were purchased from Sigma-Aldrich (Adana, Turkey) products. All of the application solutions were created from chemical reagents of analytical grade with distilled water, and they were used without extra purification. A freshly prepared solution was used for each application. Experiments were carried out under static conditions and exposed to the air. The temperature applications were performed at 25 °C (within ±1 °C) with temperature control of the cell.

2.3. Electrochemical measurements

Electrochemical measurements were carried out by using A CHI 604 model electrochemical analyzer (serial number: 6A721A) under computer control. The cell which has a double-wall one-compartment with three electrode configurations was used. While A platinum sheet with 2 cm^2 surface area was used as an auxiliary electrode, Ag/AgCl (3 M KCl) electrode was used as the reference electrode. All potentials in this study were conducted in accordance with this reference electrode. All polarization plots were carried out potentiodynamically with the scan rate of 0.001 V s^{-1} between potential ranges from −0.80 V (Ag/AgCl) to −0.20 V (Ag/AgCl). The electrochemical impedance spectroscopy measurements were carried out by applying alternating current signal of 0.005 V peak-to-peak in the frequency range of 100 kHz–0.003 Hz at open circuit potential. In the linear polarization resistance (LPR) measurements, the potential was scanned with the scan rate of 0.001 V s^{-1} from −0.010 V more cathodic potential than open circuit potential to +0.010 V nobler direction. Polarization plots were carried out in the absence and presence of 1.0×10^{-1} mM DPTH at different temperatures (298–328 K) to investigate the mechanism of inhibition and determine the activation energies of the corrosion process. In order to obtain potential of zero charge of MS, the Nyquist measurements of MS were obtained at various potentials in 0.1 M HCl solution containing 0.1 mM DPTH.

2.4. Computational details

The theoretical study was performed using the Density Functional Theory (DFT) with the B3LYP/6-311++G (d, p) basis set in Gaussian 09 and Gaussview 5.0 visualization programs [23]. The bond length, bond angle, the highest occupied molecular orbital energy (E_{HOMO}), the lowest unoccupied molecular orbital energy (E_{LUMO}), energy gap (ΔE) between LUMO and HOMO, dipole moment, Mulliken and NBO charges [24] of DPTH were calculated in water phase.

3. Results and discussion

3.1. Potentiodynamic polarization measurements

The potentiodynamic polarization curves of MS in 0.1 M HCl solutions with various concentrations of DPTH are shown in Fig. 2. The corrosion potential shifts towards negative direction with increasing DPTH concentration. The cathodic current potential curves in Fig. 2 are seen to be substantially parallel to each other as the inhibitor concentration increases. It shows that the hydrogen evolution reaction is an activation controlled reaction. The mechanism of the hydrogen evolution process is not affected by the presence of DPTH [25,26]. However, the anodic polarization curve does not display a broad linear Tafel region in the applied potential range. In the anodic part of polarization curves, the current density decreases in a wide-range potential by the addition of the DPTH. In addition to this situation, the current versus potential characteristics does not markedly change the presence of DPTH at over-voltages higher than about −0.320 V (vs Ag/AgCl). This potential is usually defined as desorption potential (E_d), which means that the adsorption mode of an inhibitor depends on the electrode potential [27]. The behaviors of DPTH may be the result of significant dissolution of iron at potentials higher than E_d, leading to the desorption rate of DPTH molecule higher than its adsorption rate. Thus, in this case, the formation of a protective film at the metal surface relies on the potential [28].

The electrochemical parameters such as corrosion potential (E_{corr}), corrosion current density (i_{corr}), and inhibition efficiency (η) were calculated and given in Table 1. It is clear from Table 1 that the corrosion current density decreases while η is rising with increasing inhibitor concentration and this indicates that DPTH adsorbs on the metal surface and hence, occurs inhibition [29]. The η was calculated according to the following equation:

$$\eta\% = \left(\frac{i_{corr} - i'_{corr}}{i_{corr}}\right) \times 100 \quad (1)$$

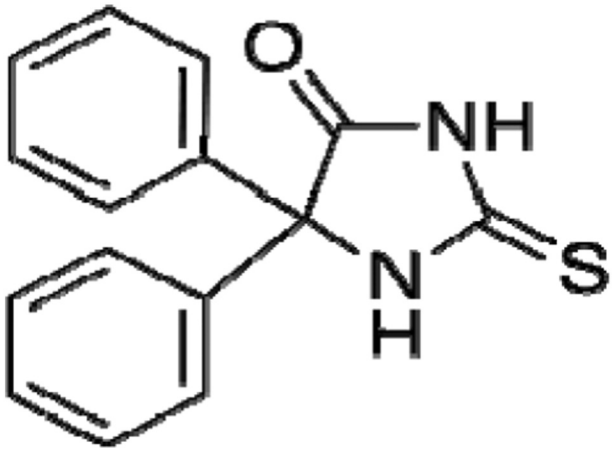

Fig. 1. Chemical structures of DPTH.

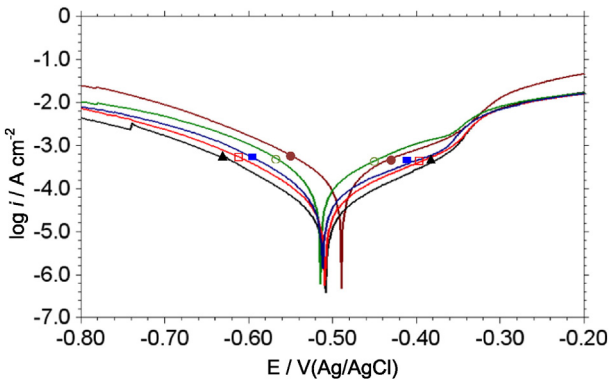

Fig. 2. Polarization curves of MS in 0.1 M HCl(●) containing various concentrations (0.005 mM (○), 0.01 mM(■), 0.05 mM (□), 0.1 mM (▲)) of DPTH at 298 K.

Table 1
Electrochemical parameters for MS determined from polarization measurements.

C_{inh}(mM)	E_{corr} (V, Ag/AgCl)	i_{corr} (mA cm^{-2})	Corrosion rate (mm year^{-1})	η (%)
Blank	−0.511	0.376	8.719	
0.005	−0.512	0.055	1.275	85
0.01	−0.513	0.028	0.649	93
0.05	−0.509	0.024	0.556	94
0.1	−0.508	0.019	0.440	95

where i_{corr} and i'_{corr} are corrosion current densities in the absence and presence of the inhibitor, respectively, obtained from extrapolation of cathodic current-potential curves to corrosion potential.

Furthermore, it is seen from Fig. 2 that the current density decreases in anodic and cathodic portions with the increasing DPTH concentration which indicates that the DPTH protective film suppresses the anodic and cathodic reactions on the MS surface. On the basis of results, DPTH for MS in 0.1 M HCl solution could be accepted as a mixed-type inhibitor.

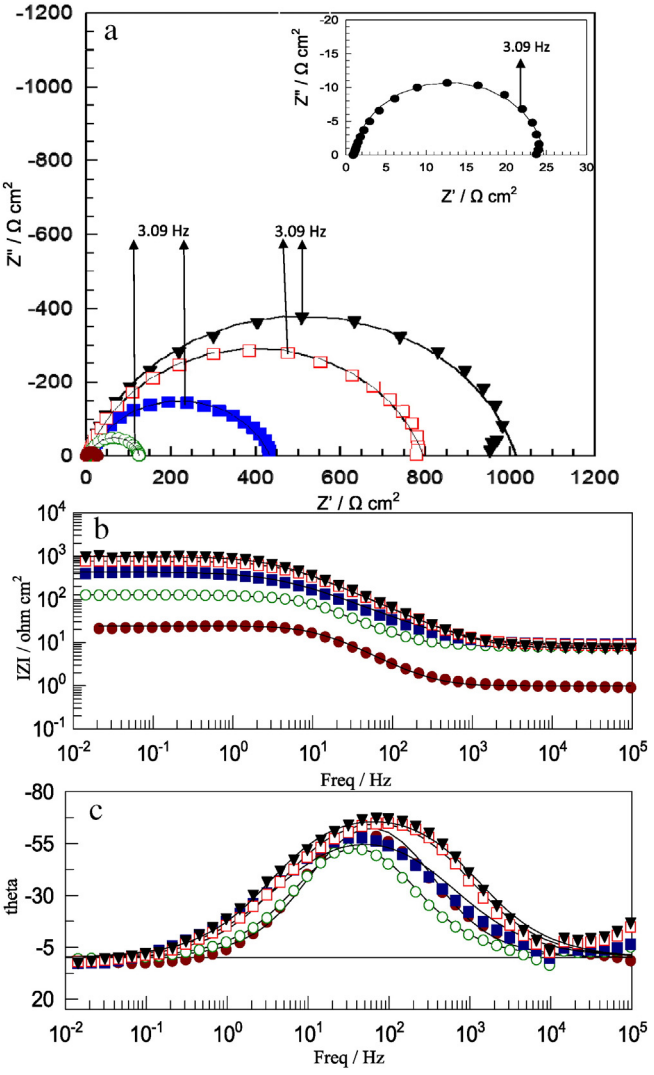

Fig. 3. Nyquist plot (a), bode (b) and phase angle (c) diagrams of MS electrode obtained in 0.1 M HCl(●) solution containing various concentrations (0.005 mM(○), 0.01 mM(■), 0.05 mM(□), 0.1 mM(▲)) (a) of DPTH.

3.2. Electrochemical impedance spectroscopy measurements

Nyquist plots of MS in uninhibited and inhibited acid solutions containing various concentrations of DPTH after 1 h of immersion time are shown in Fig.3. Nyquist's plots consisting of one depressed semi-circular shape in inhibited, and uninhibited acid solutions are seen in Fig. 3. This indicates that the corrosion of the MS in the presence and absence of inhibitor and mainly controlled by a charge transfer process [30]. By increasing concentration of DPTH in 0.1 M HCl solution, it causes a change in both shape and size of the Nyquist plots. The one depressed semicircular shape appearing in the Nyquist plots is attributed to the charge transfer resistance and the diffuse layer resistance, at low frequencies related to the adsorption of inhibitor molecules on the metal surface and all other accumulated kinds at the metal/solution interface (inhibitor molecules, corrosion products, etc.) [31]. In the evaluation of Nyquist plots, the difference between real impedance at lower and higher frequencies is commonly accepted as a charge transfer resistance. In this study, the polarization resistance (R_p) is used instead of the charge transfer resistance [32]. As in Fig. 3, the increasing R_p values with increasing concentration of the DPTH indicates the formation of a protective film at the metal surface and a barrier for the mass and the charge transfers [33].

A suitable equivalent circuit diagram is given where R_s is solution resistance, and *CPE* is a constant phase element in Fig. 4 fitting well with the experimental results by analyzing the EIS data. The Nyquist plots are not perfect semicircles as expected from the theory of EIS. Therefore, it is necessary to use the constant phase element, *CPE*, instead of double layer capacitance C_{dl} to give a more accurate fitting [34]. On the other hand, the use of a *CPE* is required as a result of inhomogeneities like the surface roughness/porosity, adsorption, or diffusion [35]. *n* is the phase shift expressed as a degree of surface inhomogeneities. The fitted data of impedance plots are given in Table 2. It can be seen from Table 2 that while R_p values obtained from EIS and LPR measurements increase with the increasing concentration of DPTH, *CPE* values decrease. The decrease in the *CPE* could be the result in a decrease in local dielectric constant and/or an increase in the thickness of double layer due to the adsorption of DPTH molecules at the metal/solution interface [36]. The inhibition efficiency (η) values obtained from the LPR measurements are comparable and in parallel with those obtained from the EIS measurement. The inhibition efficiency (η) was calculated from the polarization resistance using the following equation;

$$\eta(\%) = \left(\frac{R'_p - R_p}{R'_p}\right) x100 \qquad (2)$$

where R_p and R'_p are the polarization resistance in the absence and presence of the inhibitor, respectively.

3.3. Adsorption isotherm, activation energy and thermodynamic parameters

The interaction between the metal surface and the organic molecules is expressed by adsorption isotherms. Adsorption of organic

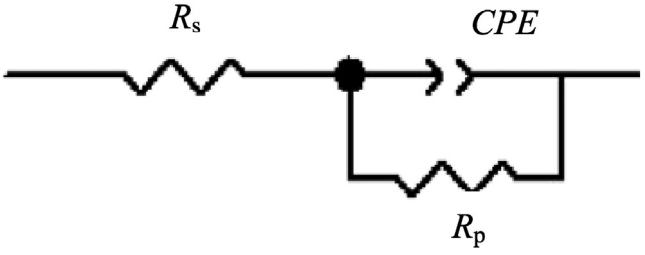

Fig. 4. Electrical equivalent circuit model used for the modeling metal/solution interface (R_p: polarization resistance, R_s: solution resistance, *CPE*: constant phase element).

Table 2
Electrochemical parameters for MS electrode corresponding to the EIS and LPR data in 0.1 M HCl solution in the absence and presence of various concentrations containing DPTH.

C_{inh} (mM)	EIS				LPR	
	R_p (Ω cm^2)	*CPE* (μF cm^{-2})	*n*	η (%)	R_p (Ω cm^2)	η (%)
Blank	24	1831	0.91		21	
0.005	118	710	0.87	79	128	83
0.01	413	656	0.80	94	385	94
0.05	790	565	0.82	96	715	97
0.1	1010	339	0.80	97	989	97

molecules on a metal surface is a substitution process between the water molecules at the metal surface and DPTH molecules in the electrolyte solution [37]. The adsorption of the inhibitors on the MS depends on the degree of surface coverage (θ). The degree of surface coverage (θ) at different concentrations of the inhibitors on the corrosion of MS was calculated from EIS results (Table 2). The best fit among the tested various isotherms was obtained with the use of the Langmuir adsorption isotherms (Fig. 5), which may be expressed by the following equation:

$$\frac{C_{inh}}{\theta} = \frac{1}{K_{ads}} + C_{inh} \quad (3)$$

where C_{inh} is inhibitor concentration, and K_{ads} is equilibrium constant of adsorption.

The plots of C_{inh}/θ versus C_{inh} show the expected linear relationship for DPTH in Fig. 5. The K_{ads}, obtained from linear equation of the straight line is 7.4×10^3 for DPTH. The Langmuir isotherm indicates that one monolayer of DPTH molecule is formed on the metal surface [38].

Based on the Langmuir isotherm, the standard free energy of adsorption (ΔG°_{ads}) can be estimated by the following equation:

$$\Delta G^o_{ads} = -RT \ln(55.5 K_{ads}) \quad (4)$$

where R is the universal gas constant and *T* is the absolute temperature. According to Eq. (4), ΔG°_{ads} was calculated as −32.1 kJ mol^{-1} at 298 K, which suggested that the adsorption of inhibitor molecules is not merely physisorption and it may include a comprehensive adsorption (physical and chemical adsorption). However, the adsorption of inhibitor molecules on the metal surfaces cannot be accepted as completely physical or chemical phenomenon. In fact, there is no clear boundary between the physical and chemical adsorption. In general, physisorption is recognized as the first step of chemical adsorption [41]. Namely, besides physical adsorption, chemical adsorption can also be possible for adsorption of DPTH molecules on MS surface. ΔG°_{ads} value obtained in this study indicates that the inhibitor adsorbs on the metal surface both physically and chemically, but physisorption is the predominant mode of adsorption [39–42].

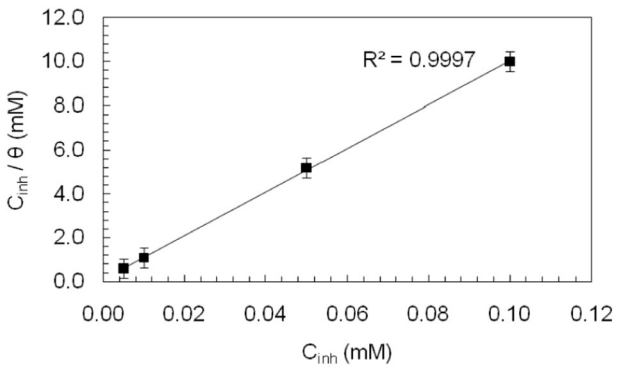

Fig. 5. Langmuir adsorption plot for the MS electrode in 0.1 M HCl containing different concentrations of DPTH.

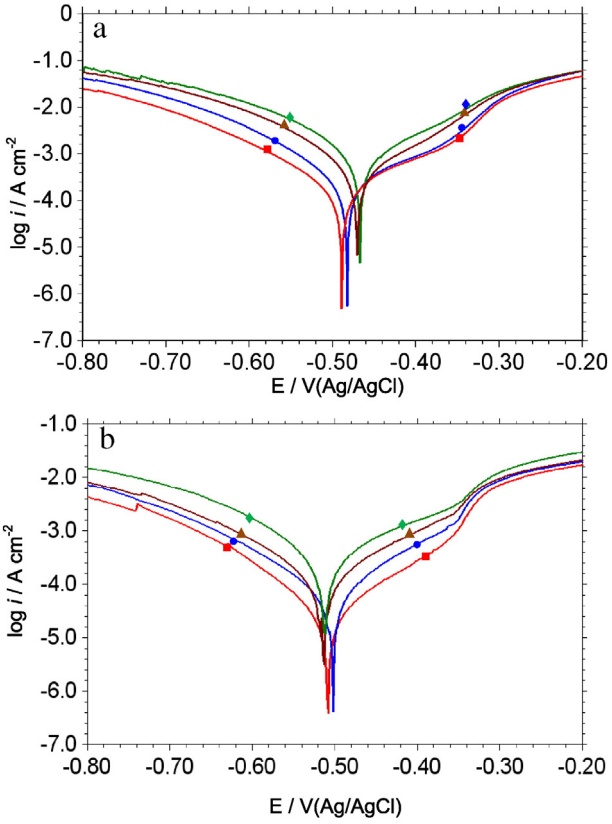

Fig. 6. Polarization curves of MS in 0.1 M HCl (a) and 0.1 mM DPTH (b) at various temperatures (298 K (■), 308 K (●), 318 K (▲), 328 K (♦)).

Potentiodynamic polarization measurements were performed to determine the activation energy of the corrosion process and the inhibition behavior of DPTH in the temperature range of 298–328 K in 0.1 M HCl solution in the absence and presence of 0.1 mM DPTH (Fig. 6). As seen from Fig.6, the current density values are increased with the increasing temperature in the absence and presence of 0.1 mM DPTH in 0.1 M HCl solution. In acidic media, corrosion of metal usually accelerates due to the higher dissolution rate of the MS with the rise in temperature. The decrease in the current density values in the presence of DPTH might be due to the weakening of adsorbed inhibitor molecules on the MS surface. The effect of temperature on corrosion rate can be expressed by the Arrhenius equation:

$$i_{corr} = A \exp\left(\frac{-E_a}{RT}\right) \quad (5)$$

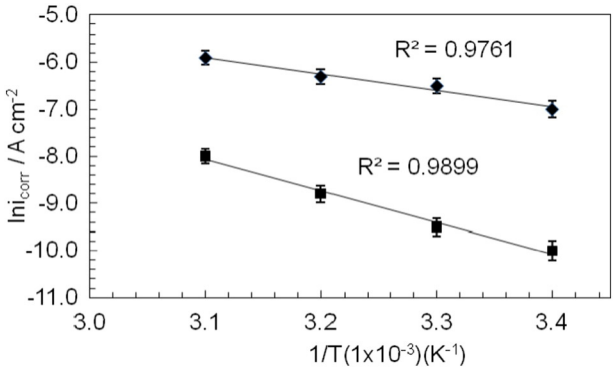

Fig. 7. Arrhenius plots for the MS electrode in 0.1 M HCl (♦) and containing 0.1 mM DPTH (■) solutions.

where E_a is the activation energy of the corrosion process, T is the temperature, R is the gas constant, A is the Arrhenius constant and i_{corr} is corrosion current density. Arrhenius plots of the logarithm of the current density against reciprocal of temperature in the absence and presence of 0.1 mM DPTH are shown in Fig. 7. The values of activation energy in the absence and presence of the inhibitor were obtained from the slope (E_a/R) of two straight lines and their values were determined as 29.1 kj mol^{-1} K^{-1}, 55.7 kJ mol^{-1} K^{-1}, respectively. The value of E_a in the presence of the inhibitor is greater than in the absence of the inhibitor. The increase of E_a in the presence of the inhibitor indicates that the corrosion reaction decreased due to the adsorption of inhibitor molecules on the MS surface [43,44].

The heat of adsorption (Q_{ads}) can be calculated according to the following equation:

$$\frac{\theta}{1-\theta} = AC\exp\left(-\frac{Q_{ads}}{RT}\right) \tag{6}$$

where R is the gas constant, A is constant, C is inhibitor concentration, Q_{ads} is the heat of adsorption and equal to enthalpy of adsorption process (ΔH°_{ads}) with good approximation because pressure is constant, T is the temperature, θ is the surface coverage of the inhibitor molecules. A plot of log ($\theta/(1-\theta)$) versus $1/T$ shows a linear line. The slope of the straight line is $-Q_{ads}$/R and equal to ΔH°_{ads} value. ΔH°_{ads} value was calculated as −32.1 kJ mol^{-1} K^{-1}. The ΔH°_{ads} indicates that the adsorption of DPTH molecules is an exothermic process [45] and η decreases with increasing temperature. This situation can be explained on the basis that the adsorbed inhibitor molecules on the MS surface is more desorption at higher temperature and the value of ΔH°_{ads} is lower than 40 kJ mol^{-1} for physisorption process while for chemisorption it is about 100 kJ mol^{-1} [46].

The entropy of adsorption process (ΔS°_{ads}) concerning the adsorption of DPTH on MS was also calculated from the thermodynamic basic equation:

$$\Delta G^{o}_{ads} = \Delta H^{o}_{ads} - T\Delta S^{o}_{ads}. \tag{7}$$

The ΔS°_{ads} value obtained from Eq. (7) is −2.01 J mol^{-1} K^{-1}. The sign of ΔS°_{ads} was found as negative, thus inhibitor molecules easily moving in the bulk solution were adsorbed in an orderly manner onto the MS, leading to a decrease in entropy [47,48].

3.4. Potential of zero charge

The process of adsorption is influenced by factors such as the nature and surface charges on the metal, the type of aggressive electrolyte, the chemical structure of inhibitor and the nature of its interaction with the metal surface. The surface charge of metal is determined by the position of corrosion potential E_{corr} regarding the appropriate potential of zero charge (PZC). The EIS data with the double-layer capacitance (C_{dl}) versus voltage (E) plots [49–52] was used to determine the PZC. Generally, a minimum value on the C_{dl} versus the applied potential curve is considered as the PZC of the electrode, and then the surface net charge of metal can be evaluated in a given aggressive medium according to the difference $E_r = E_{corr} - PZC$, where E_r is the Antropov's "rational" corrosion potential [51].

The dependence of C_{dl} on the applied potential of MS in 0.1 M HCl with the addition of 0.1 mM DPTH after 1 h of immersion time is given in Fig. 8. According to Fig. 8, PZC is the minimum point of parabola and its potential value is −0.523 V (Ag/AgCl). According to the PZC, E_r is positive and its potential is −0.493 V (Ag/AgCl). For this reason, the MS surface is positively charged at its corrosion potential.

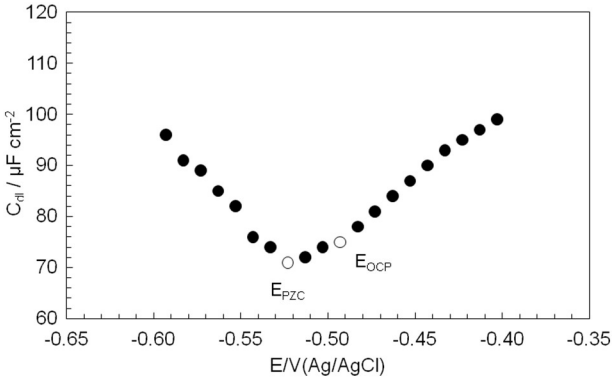

Fig. 8. The plot of C_{dl} vs. applied potential in 0.1 M HCl containing 0.1 mM DPTH.

3.5. Inhibition mechanism

The inhibition mechanism of inhibitor molecules was offered as; the DPTH can also be adsorbed on the steel surface via electrostatic interaction between the positively charged metal surface and the charged inhibitor molecules in Cl^- containing aggressive medium. The anodic reactions;

$$Fe + Cl^- \leftrightarrow (FeCl^-)_{ads} \tag{8}$$

$$(FeCl^-)_{ads} \leftrightarrow (FeCl)_{ads} + e^- \tag{9}$$

$$(FeCl)_{ads} \leftrightarrow FeCl^+ + e^- \tag{10}$$

$$FeCl^+ \leftrightarrow Fe^{2+} + Cl^-. \tag{11}$$

In acid solution, the DPTH is available in the form of protonated (cations);

$$DPTH + H^+ \leftrightarrow DPTHH^+. \tag{12}$$

It is known that the chloride ions have a small degree of hydration, and due to specific adsorption, they should be first adsorbed on the positively charged metal surface which is determined from PZC results. They could form a negative excess charge towards its solution side and favor more adsorption of the positively charged inhibitor molecules in solution. Hence, in the case of the inhibitor present, the cationic $DPTHH^+$ molecules can be easily adsorbed on MS surface via electrostatic interaction with the adsorbed Cl^- ions which form interconnecting bridges between the positively charged MS surface and cation of DPTH [52,53]. In addition to the above physical adsorption, the adsorption of DPTH molecules can occur directly through sharing lone pair electrons in hetero atoms and/or p electrons in phenyl rings with the unoccupied d orbital of iron atoms to form coordinate covalent bond (chemisorption).

Furthermore, the protonated inhibitor molecules may affect the cathodic reaction. In acid solution, the cathodic hydrogen evolution reaction may be given as follow:

$$Fe + H^+ \leftrightarrow (FeH^+)_{ads} \tag{13}$$

$$(FeH^+)_{ads} + e^- \rightarrow (FeH)_{ads} \tag{14}$$

$$(FeH)_{ads} + H^+ + e^- \rightarrow Fe + H_2. \tag{15}$$

The $DPTHH^+$ molecules may adsorbed at cathodic sites of mild steel in competition with hydrogen ions that reduce to H_2 gas [54].

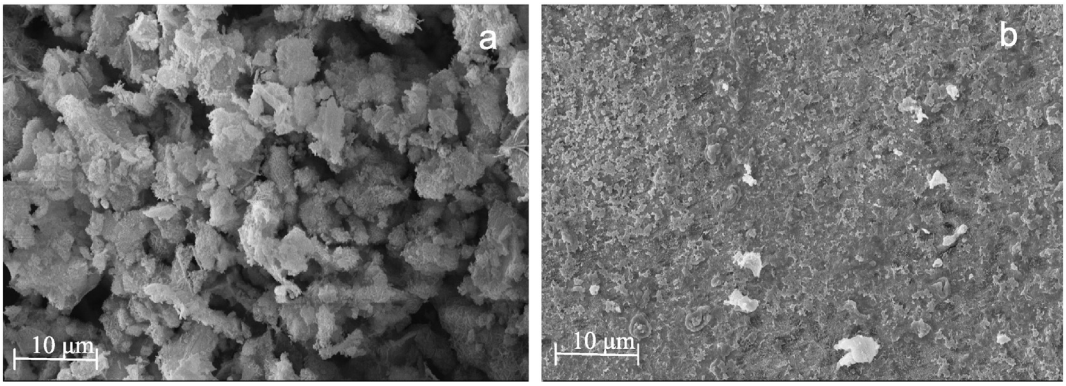

Fig. 9. SEM images of MS surface after 120 h immersion in 0.1 M HCl solution in the absence (a) and presence of 0.1 mM DPTH (b).

3.6. SEM analysis

Fig. 9 shows the surface morphology of the MS in the absence and in the presence of 0.1 mM DPTH in 0.1 M HCl solution after 120 h at 298 K. The MS electrode is immersed in 0.1 M HCl solution in the absence of DPTH (Fig. 9a). It can be seen that some cracks, spheres and pits form on the MS surface due to attack of corrosive solution. The MS surface in the presence of the inhibitor (Fig. 9b) is well protected, and it has a smooth surface. The corrosion of MS is prevented due to the protective adsorption film formed on the MS surface. Therefore, it can be concluded that DPTH shows a good inhibition performance for the corrosion of MS in acidic solution.

3.7. Theoretical calculations

The optimized structure parameters of DPTH are given in Table 3. The calculated values were compared with literature [55,56]. The C1 N4 bond length was 1.324 Å. Aleksander Roszak et al. [55] determined the value as 1.326 Å. The variation in the bond lengths of C1 N7 and C1 N4 may have more to do with increase electron density around C3 and N4 due to electron donating effect of the phenyl group. The C1 S31 bond length was 1.734 Å, the C2 O8 bond length was also 1.202 Å which was usual for thiocarbonyl and carbonyl groups [53,55]. The N4 C1 N7 bond angle was 107.856°, which was higher than C2 C3 N4 bond angle (almost 99°) on account of the phenyl groups on C3. Analysis of Table 3 shows that the calculated bond lengths and angles are consistent with literature [55]. The thiohydantoin ring geometry of 5-benzyl-2-thiohydantoin was investigated by Deval et al. [56] the CS bond length was 1.635 Å and C = O was 1.206 Å for optimized monomer molecule and values were almost parallel with experimental results [57].

The Mulliken and NBO charges are given in Table 4. The total negative Mulliken charge was −5.097. The highest negative charge was located on S31 atom which was almost −0.8. The total negative NBO charge was −2.581. The NBO charges distribution showed that the highest negative charge was located on N7 atom. It should be noted that inhibitor molecules adsorb mainly through electrostatic interactions between the negatively charged atoms and the positively charged metal surface (physisorption) [58]. The higher negative charge was located on thiohydantoin ring, therefore adsorption may occurred on N7 and S31 terminal of thiohydantoin ring in DPTH. According to literature [55], hydrogen bond should form between O and the H atom binding with N atom and molecules connected by hydrogen bonds should form ribbon-like infinite sheets. After forming first adsorption layer, it may form other layers by accumulation of DPTH with hydrogen bonds. For detailed information, the stabilization energy $E^{(2)}$ was determined by the NBO calculations with the second-order Fock matrix which was carried out for each donor (i) and acceptor (j), in order to understand intramolecular bonding and interaction among bonds. The $E^{(2)}$ values of nS31 → σ* C1 N4 was 13.40 kcal mol^{-1}, nS31 → σ* C1 N7 was 14.31 kcal mol^{-1} and nO8 → σ* C2 N7 was 1.41 kcal mol^{-1} in water

Table 3
The bond length and bond angle of DPTH in water phase.

Bond length (Å)	Water phase	Reference*
C1 N4	1.324	1.326
C1 N7	1.360	1.464
C1 S31	1.734	1.648
C2 N7	1.384	1.392
C2 O8	1.202	1.216
Bond angle (°)		
N4 C1 N7	107.856	106.790
N7 C1 S31	124.893	124.460
N7 C2 O8	126.536	126.700
C2 C3 N4	99.721	99.930

Table 4
The calculated Mulliken and NBO charges of DPTH.

Atoms	Mulliken	NBO
C1	0.32194	0.47810
C2	−0.11142	0.84061
C3	0.87873	0.06680
N4	0.05248	−0.69409
H5	0.34667	0.48414
H6	0.39937	0.49180
N7	−0.15397	−0.76376
O8	−0.31764	−0.60726
C9	0.41365	−0.07525
C10	−0.35298	−0.21498
C11	−0.36592	−0.22028
C12	−0.32477	−0.24261
H13	0.20572	0.26304
C14	−0.52821	−0.24062
H15	0.21850	0.25133
C16	−0.44021	−0.22905
H17	0.21264	0.25687
H18	0.21680	0.25781
H19	0.18412	0.25619
C20	0.82943	−0.07784
C21	−0.30344	−0.21961
C22	−0.32634	−0.22313
C23	−0.39982	−0.24214
H24	0.19790	0.25813
C25	−0.32168	−0.24150
H26	0.20793	0.26303
C27	−0.47615	−0.23343
H28	0.21610	0.25636
H29	0.21059	0.25653
H30	0.18272	0.25537
S31	−0.87271	−0.41057

phase. The maximum energy delocalization occurred between nS31 → σ ∗ C1 N7 which was affected from configuration of molecule.

The HOMO and LUMO energy values give further insights which are related with the electron donating and accepting ability of a molecule, respectively. The donation forms normal covalent bonds and accepting forms the back donation covalent bonds [59]. The E_{HOMO} was −6.668 eV in water phase analysis, which indicates a tendency of the molecule to donate electrons to the appropriate acceptor. The low E_{LUMO} value (−1.794 eV) demonstrated that the electron accepting ability of the molecule was higher. The energy gap between LUMO and HOMO (ΔE) was 4.875 eV. It reflects the higher inhibition efficiency of DPTH because the lower ΔE causes the, improvement on the reactivity of the molecule, which facilitates adsorption [60,61]. Furthermore, the higher dipole moment (5.152 Debye) proved that the dipole–dipole interaction of DPTH and metal surface was higher. The fraction of electrons (ΔN) transferred from DPTH was 0.745 in water phase. The value was high enough when compared with literature [9,62–64]. It supported the high inhibition efficiency of DPTH. Furthermore, the localization of HOMO and LUMO orbital correlates it. The spread of orbital is not even on the entire molecule. In Fig. 10, it was seen that main locations of orbital were on the S, N and O atoms as expected in the literature [51].

Theoretical results showed that DPTH was most probably adsorbed on S31 atom to MS surface and it may connect with other DPTH molecules via hydrogen bonds in aqueous solution. Therefore, calculations which were obtained in water phase were correlated with the experimental results.

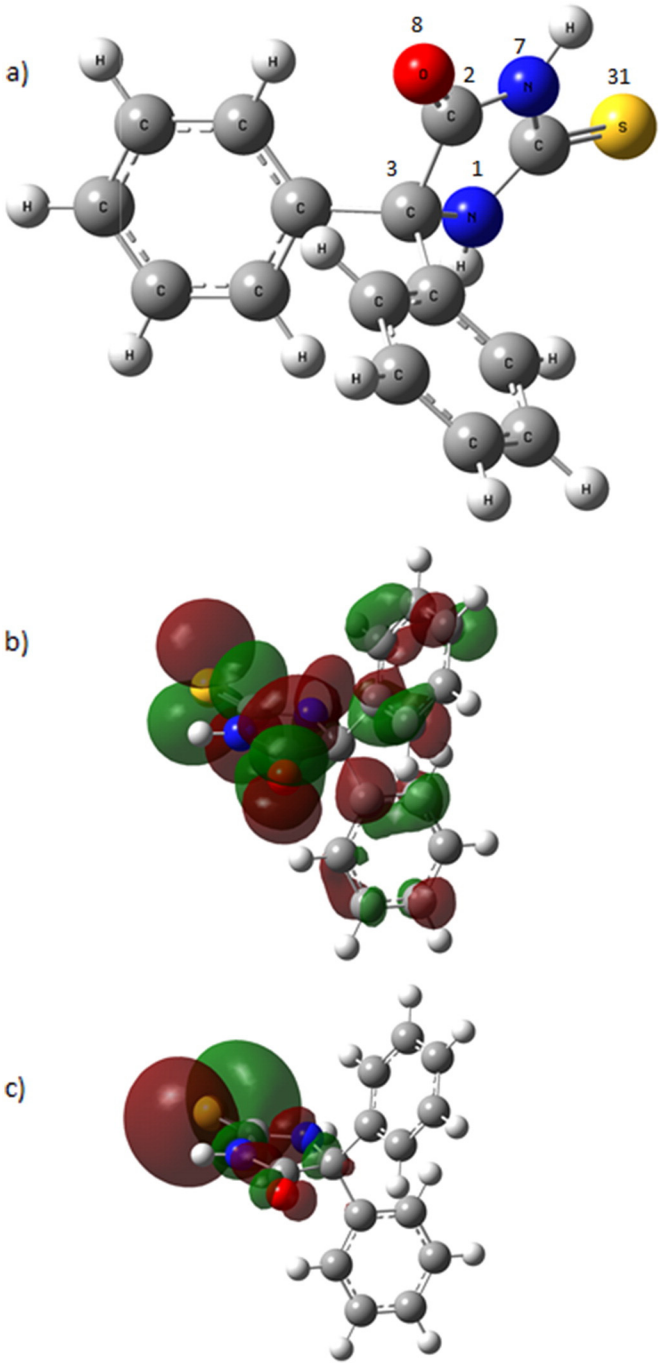

Fig. 10. The optimized structure of DPTH (a) and HOMO (b), LUMO (c) orbitals.

3.8. Comparison of similar molecules in literature

4,5-Diphenyl-1H-imidazole-2-thiol (DIT), 3,5-diphenyl-4H-1,2,4-triazole (DHT) and 2-Thiohydantoin (2-THD) structures are given in Fig 11 to compare with DPTH. These are chosen as similar to DPTH due to the phenyl groups and heteroatoms like N, O, S found in their structure. It is observed that the inhibition efficiency of these molecules was over 90% as in DPTH. DIT from these molecules has been evaluated as a corrosion inhibitor in 1 M HCl (Fig. 11 a). Its inhibition efficiency was determined as 91% by weight loss technique in the presence of 1.0×10^{-2} M DIT in 1 M HCl. In a similar way to DPTH, the high inhibition efficiency of DIT was attributed to aromatic π-electrons and unshared electrons pairs on the nitrogen and sulfur atoms interacting with vacant d-orbitals of iron as well as physical adsorption [65,66]. Comparison of the quantum chemical parameters of the DPTH with DIT showed that; DIT has lower dipole moment than DPTH, which is 4.904 Debye. The high value of dipole moment implies the strong adsorption of molecule at the electrode surface, so DPTH has higher inhibition efficiency than DIT. The HOMO and LUMO energies of DIT are −1.381 eV and −1.026 eV, respectively and these orbitals are placed on S and N atoms.

DHT given in Fig. 11b shows 98.5% inhibition efficiency in 1 M HCl from EIS results. The inhibition efficiency for DHT can be explained with intramolecular hydrogen bonding among DHT molecules from the XPS studies. This event is related to increase of the binding energy and on the basis of donor–acceptor interactions between the unshared electrons pairs on the nitrogen atoms, the π-electrons of the phenyl groups and the vacant d orbitals of metal surface atoms. Additionally, X-ray photoelectron spectroscopy (XPS) showed that inhibition of corrosion by DHT is due to the formation of a chemisorbed film on the steel surface [66]. The pictorial representation of the HOMO and LUMO orbitals of DHT was located phenyl groups and N atoms. The DPTH has larger HOMO surface than DHT and the total negative Mulliken charge of DHT is lower than DPTH, which is −1.872. The highest negative charge is located on N atom and the value is −0.63. The theoretical calculation of DHT supports XPS results.

The corrosion performance of 2-thiohydantoin (2-THD) has been investigated in 0.1 M HCl (Fig. 11 c) [19] and it has been observed from EIS results that DPTH has nearly the same inhibition efficiency as 2-THD (1.0×10^{-2} M) at 100 times lower concentration, in the same acid solution. DPTH has two phenyl groups which are different from 2-THD. It is determined that the adsorption on the MS surface of both molecules is the chemisorption as well as predominantly physical adsorption. The highest negative charge of 2-THD is located on N atom, which is −0.91 and molecule may adsorbed on electrode surface by unshared electron pair of amine group. The high inhibition efficiency of DPTH at low concentration can be explained by the contribution to adsorption on MS surface of π electrons in phenyl groups of DPTH molecules compared to 2-THD. It is described by two shapes of adsorption, through the free lone pairs on nitrogen and sulfur atoms as well as π-electrons of the phenyl rings and protonated species from sulfur atom of DPTH and 2-THD form cations which are electrostatically attracted to the

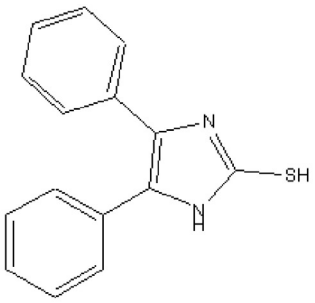

a) 4,5-Diphenyl-1H Imidazole-2-Thiol (DIT)

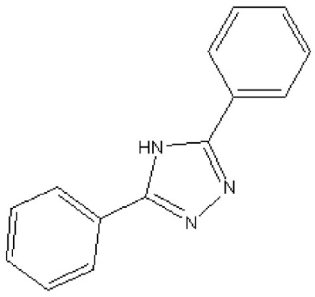

b) 3,5-diphenyl-4*H*-1,2,4-triazole (DHT)

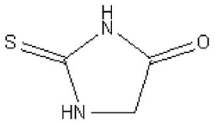

c) 2–Thiohydantoin (2–THD)

Fig. 11. The similarity molecules to DPTH.

pre-adsorbed Cl^{-1} anion on the MS surface. In addition, DPTH molecules may also be stabilized by the intramolecular hydrogen bonds [54]. The increase in inhibition efficiency for DPTH can be due to intramolecular forces [19].

4. Conclusion

The following results can be plotted from this work:

1) The corrosion rate of MS in 0.1 M HCl, decreases upon the addition of the minimal concentration of DPTH (0.005–0.1 mM) and inhibition efficiency increases with increasing DPTH concentration.
2) The DPTH acts as a mixed type inhibitor, it suppresses both anodic and cathodic reactions, adsorption of DPTH increases with decreasing temperature.
3) The DPTH has high dipole moment which allows strong interaction with electrode surface and the highest negative charge is located on N and S atoms of DPTH, therefore adsorption may occur on N-heterocyclic ring by electrostatic interactions.
4) The location of the frontier molecular orbitals (HOMO and LUMO) and NBO analysis indicate that DPTH may be connected by hydrogen bonds which form ribbon-like infinite sheets and adsorb through the active centers N and S atoms and π electrons.

Acknowledgments

The authors are greatly thankful to Cukurova University Research Fund (Project Number: FEF2013BAP10).

Appendix A. Supplementary data

Supplementary data to this article can be found online at http://dx.doi.org/10.1016/j.molliq.2016.02.087.

References

[1] A.O. Odiongenyi, S.A. Odoemelam, N.O. Eddy, Corrosion inhibition and adsorption properties of ethanol extract of *Vernonia amygdalina* for the corrosion of mild steel in H_2SO_4, Port. Electrochim. Acta 27 (2009) 33–45.
[2] E.E. Ebenso, N.O. Eddy, A.O. Odiongenyi, Corrosion inhibition and adsorption properties of methocarbamol on mild steel in acidic medium, Port. Electrochim. Acta 27 (2009) 13–22.
[3] H. Choi, Y. Kyun Song, K. Young Kim, J. Myung Park, Encapsulation of triethanolamine as organic corrosion inhibitor into nanoparticles and its active corrosion protection for steel sheets, Surf. Coat. Technol. 206 (2012) 2354–2362.
[4] M. Palomar-Pardave, M. Romero-Romo, H. Herrera-Hernandez, M.A. Abreu- Quijano, Natalya V. Likhanova, J. Uruchurtu, J.M. Juarez-Garcia, Influence of the alkyl chain length of 2 amino 5 alkyl 1,3,4 thiadiazole compounds on the corrosion inhibition of steel immersed in sulfuric acid solutions, Corros. Sci. 54 (2012) 231–243.
[5] Y.P. Khodyrev, E.S. Batyeva, E.K. Badeeva, E.V. Platova, L. Tiwari, O.G. Sinyashin, The inhibition action of ammonium salts of O,O-dialkyldithiophosphoric acid on carbon dioxide corrosion of mild steel, Corros. Sci. 53 (2011) 976–983.
[6] S.K. Shukla, M.A. Quraishi, E.E. Ebenso, Adsorption and corrosion inhibition properties of cefadroxil on mild steel in hydrochloric acid, Int. J. Electrochem. Sci. 6 (2011) 2912–2931.
[7] X. Wang, H. Yang, F. Wang, An investigation of benzimidazole derivative as corrosion inhibitor for mild steel in different concentration HCl solutions, Corros. Sci. 53 (2011) 113–121.
[8] A.Y. Musa, A.A.H. Kadhum, A.B. Mohamad, M.S. Takrıff, A.R. Daud, S.K. Kamarudın, Adsorption isotherm mechanism of amino organic compounds as mild steel corrosion inhibitors by electrochemical measurement method, J. Cent. S. Univ. Technol. 17 (2010) 34–39.
[9] A. Doner, R. Solmaz, M. Ozcan, Gulfeza Kardas, Experimental and theoretical studies of thiazoles as corrosion inhibitors for mild steel in sulphuric acid solution, Corros. Sci. 53 (2011) 2902–2913.
[10] M.K. Awad, M.R. Mustafa, M.M.A. Elnga, Computational simulation of the molecular structure of some triazoles as inhibitors for the corrosion of metal surface, J. Mol. Struct. THEOCHEM 959 (2010) 66–74.
[11] D. Asefi, M. Arami, N.M. Mahmoodi, Electrochemical effect of cationic geminisurfactant and halide salts on corrosion inhibition of low carbon steel in acidmedium, Corros. Sci. 52 (2010) 794–800.
[12] R.M. Issa, M.K. Awad, F.M. Atlam, Quantum chemical studies on the inhibition of corrosion of copper surface by substituted uracils, Appl. Surf. Sci. 255 (2008) 2433–2441.
[13] X.H. Li, G.N. Mu, Tween-40 as corrosion inhibitor for cold rolled steel in sulphuric acid: weight loss study, electrochemical characterization, and AFM, Appl. Surf. Sci. 252 (2005) 1254–1265.
[14] Z. Tao, S. Zhang, W. Li, B. Hou, Adsorption and corrosion inhibition behavior of mild steel by one derivative of benzoic–triazole in acidic solution, Ind. Eng. Chem. Res. 49 (2010) 2593–2599.
[15] S. John, B. Joseph, K.V. Balakrishnan, K.K. Aravindakshan, A. Joseph, Electrochemical and quantum chemical study of 4-[(E)-[(2,4-dihydroxy phenyl) methylidine] amino]-6-methyl-3-sulphanylidine-2,3,4,5-tetra hydro-1,2,4-triazin-5-one [DMSTT], Mater. Chem. Phys. 123 (2010) 218–224.
[16] M.A. Quraishi, D. Jamal, Dianils, new and effective corrosion inhibitors for oilwell steel (N-80) and mild steel in boiling hydrochloric acid, Corrosion 56 (2000) 156–160.
[17] A. Fiala, A. Chibani, A. Darchen, A. Boulkamh, K. Djebbar, Appl. Surf. Sci. 253 (2007) 9347–9356;

I.B. Obot, N.O. Obi-Egbedi, S.A. Umoren, Int. J. Electrochem. Sci. 4 (2009) 863–877.
[18] J. Thanusu, V. Kanagarajan, M. Gopalakrishnan, Spectral characterization of novel bis heterocycles comprising both piperidine and thiohydantoin nuclei, Res. Chem. Intermed. 36 (2010) 1073–1084.
[19] A. Ongun Yüce, G. Kardaş, Adsorption and inhibition effect of 2-thiohydantoin on mild steel corrosion in 0.1 M HCl, Corros. Sci. 58 (2012) 86–94.
[20] S.S. Kandil, G.B. El–Hefnawy, E.A. Baker, Thermal and spectral studies of 5-(phenylazo)-2-thiohydantoin and 5-(2-hydroxyphenylazo)-2-thiohydantoin complexes of cobalt(II), nickel(II) and copper(II), Thermochim. Acta 414 (2004) 105–113.
[21] K. Kiec-Kononowicz, J. Karolak-Wojciechowska, J. Robak, Fused 2-thiohydantoin derivatives: evaluation as potential antioxidants, Arch. Pharm. 330 (1997) 85–90.
[22] T.-S. Lee, L.-C. Chen, Y. Liu, J. Wu, Y.-C. Liang, W.-S. Lee, 5,5-Diphenyl-2-thiohydantoin-N10 (DPTH-N10) suppresses proliferation of cultured colon cancer cell line COLO-205 by inhibiting DNA synthesis and activating apoptosis, N-S Arch. Pharmacol. 382 (2010) 43–50.
[23] M.J. Frisch, G.W. Trucks, H.B. Schlegel, G.E. Scuseria, M.A. Robb, J.R. Cheeseman, G. Scalmani, V. Barone, B. Mennucci, G.A. Petersson, H. Nakatsuji, M. Caricato, X. Li, H.P. Hratchian, A.F. Izmaylov, J. Bloino, G. Zheng, J.L. Sonnenberg, M. Hada, M. Ehara, K. Toyota, R. Fukuda, J. Hasegawa, M. Ishida, T. Nakajima, Y. Honda, O. Kitao, H. Nakai, T. Vreven, J.A. Montgomery Jr., J.E. Peralta, F. Ogliaro, M. Bearpark, J.J. Heyd, E. Brothers, K.N. Kudin, V.N. Staroverov, R. Kobayashi, J. Normand, K. Raghavachari, A. Rendell, J.C. Burant, S.S. Iyengar, J. Tomasi, M. Cossi, N. Rega, J.M. Millam, M. Klene, J.E. Knox, J.B. Cross, V. Bakken, C. Adamo, J. Jaramillo, R. Gomperts, R.E. Stratmann, O. Yazyev, A.J. Austin, R. Cammi, C. Pomelli, J.W. Ochterski, R.L. Martin, K. Morokuma, V.G. Zakrzewski, G.A. Voth, P. Salvador, J.J. Dannenberg, S. Dapprich, A.D. Daniels, Ö. Farkas, J.B. Foresman, J.V. Ortiz, J. Cioslowski, D.J. Fox, Gaussian 09, Revision D.01, Gaussian, Inc., Wallingford CT, 2009.
[24] NBO Version 3.1, E.D. Glendening, A.E. Reed, J.E. Carpenter, F. Weinhold.
[25] F. El-Hajjaji, B. Zerga, M. Sfaira, M. Taleb, M.E. Touhami, B. Hammouti, S.S. Al-Deyab, H. Benzeid, E.M. Essassi, Comparative study of novel N-substituted quinoxaline derivatives towards mild steel corrosion in hydrochloric acid: part 1, J. Mater. Environ. Sci. 5 (2014) 255–262.
[26] A.K. Singh, A.K. Singh, E.E. Ebenso, Inhibition effect of cefradine on corrosion of mild steel in HCl solution, Int. J. Electrochem. Sci. 9 (2014) 352–364.
[27] H. Ashassi-Sorkhabi, E. Asghari, P. Ejbari, Electrochemical studies of adsorption and inhibitive performance of basic yellow 28 dye on mild steel corrosion in acid solutions, Acta Chim. Slov. 58 (2011) 270–277.
[28] M. Lagrenee, B. Mernari, M. Bouanis, M. Traisnel, F. Bentiss, Study of the mechanism and inhibiting efficiency of 3,5-bis(4-methylthiophenyl)-4H-1,2,4-triazole on mild steel corrosion in acidic media, Corros. Sci. 44 (2002) 573–588.
[29] H. Zarrok, A. Zarrouk, R. Salghi, M. Assouag, N. Bouroumane, E.E. Ebenso, B. Hammouti, R. Touzani, H. Oudda, Corrosion and corrosion inhibition of carbon steel in hydrochloric acid solutions by 2-[bis-(3,5-dimethyl-pyrazol-1-ylmethyl)-amino]-3-hydroxybutyric acid, Pharm. Lett. 5 (2013) 327–335.
[30] H. Vashisht, S. Kumar, I. Bahadur, G. Singh, Evaluation of (2-hydroxyethyl) triphenyl phosphonium bromide as corrosion inhibitor for mild steel in sulphuric acid, Int. J. Electrochem. Sci. 8 (2013) 684–699.
[31] M. Erbil, The determination of corrosion rates by analysis of AC impedance diagrams, Chim. Acta Turc. 1 (1988) 59–70.
[32] A. Zarrouk, B. Hammouti, S.S. Al-Deyab, R. Salghi, H. Zarrok, C. Jama, F. Bentiss, Corrosion inhibition performance of 3,5-diamino-1,2,4-triazole for protection of copper in nitric acid solution, Int. J. Electrochem. Sci. 7 (2012) 5997–6011.
[33] B.M. Mıstry, N.S. Patel, S. Sahoo, S. Jauharı, Experimental and quantum chemical studies on corrosion inhibition performance of quinoline derivatives for MS in 1 N HCl, Bull. Mater. Sci. 35 (2012) 459–469.
[34] S.-J. Ding, B.-W. Chang, C.-C. Wu, M.-F. Lai, H.-C. Chang, Electrochemical evaluation of avidin–biotin interaction on self-assembled gold electrodes, Electrochim. Acta 50 (2005) 3660–3666.
[35] K.C. Emregul, R. Kurtaran, O. Atakol, An investigation of chloride-substituted Schiff bases as corrosion inhibitors for steel, Corros. Sci. 45 (2003) 2803–2817.
[36] A. Majjane, D. Rair, A. Chahine, M. Et-tabirou, M. Ebn Touhami, R. Touir, Preparation and characterization of a new glass system inhibitor for mild steel corrosion in hydrochloric solution, Corros. Sci. 60 (2012) 98–103.
[37] J.O'M. Bockris, A. K.N. Reddy, Modern Electrochemistry, vol. 2, Published by Plenum Publishing Corporation, 227 West 17th, Street, New York, 1976.
[38] M. Scendo, J. Trela, Adenine as an effective corrosion inhibitor for stainless steel in chloride solution, Int. J. Electrochem. Sci. 8 (2013) 9201–9221.
[39] A. Khamis, M.M. Saleh, M.I. Awad, B.E. El-Anadouti, Enhancing the inhibition action of cationic surfactant with sodium halides for mild steel in 0.5 M H2SO4, Corros. Sci. 74 (2013) 83–91.
[40] X. Li, S. Deng, H. Fu, X. Xie, Synergistic inhibition effects of bamboo leaf extract/major components and iodide ion on the corrosion of steel in H_3PO_4 solution, Corros. Sci. 78 (2014) 29–42.
[41] S. Deng, X. Li, X. Xie, Hydroxymethyl urea and 1,3-bis(hydroxymethyl) urea as corrosion inhibitors for steel in HCl solution, Corros. Sci. 80 (2014) 276–289.
[42] P. Kalaiselvi, S. Chellammal, S. Palanichamy, G. Subramanian, Artemisia pallens as corrosion inhibitor for mild steel in HCl medium, Mater. Chem. Phys. 120 (2010) 643–648.
[43] N.O. Obi-Egbedi, I.B. Obot, Inhibitive properties, thermodynamic and quantum chemical studies of alloxazine on mild steel corrosion in H_2SO_4, Corros. Sci. 53 (2011) 263–275.
[44] K.R. Ansari, M.A. Quraishi, Ambrish Singh, Schiff's base of pyridyl substituted triazoles as new and effective corrosion inhibitors for mild steel in hydrochloric acid solution, Corros. Sci. 79 (2014) 5–15.
[45] E.A. Noor, A.H. Al-Moubaraki, Thermodynamic study of metal corrosion and inhibitor adsorption processes in mild steel/1-methyl-4[4′(-X)-styryl pyridinium iodides/hydrochloric acid systems, Mater. Chem. Phys. 110 (2008) 145–154.
[46] I. El Ouali, B. Hammouti, A. Aouniti, Y. Ramli, M. Azougagh, E.M. Essassi, M. Bouachrine, Thermodynamic characterisation of steel corrosion in HCl in the presence of 2-phenylthieno (3, 2-b) quinoxaline, J. Mater. Environ. Sci. 1 (1) (2010) 1–8.
[47] A. Chetouani, K. Medjahed, K.E. Sid-Lakhdar, B. Hammouti, M. Benkaddour, A. Mansri, Poly(4-vinylpyridine-poly(3-oxide-ethylene) tosyle) as an inhibitor for iron in sulphuric acid at 80 °C, Corros. Sci. 46 (2004) 2421–2430.
[48] G. Mu, X. Li, G. Liu, Synergistic inhibition between tween 60 and NaCl on the corrosion of cold rolled steel in 0.5 M sulfuric acid, Corros. Sci. 47 (2005) 1932–1952.
[49] A. Lukomska, J. Sobkowski, Potential of zero charge of monocrystalline copper electrodes in perchlorate solutions, J. Electroanal. Chem. 567 (2004) 95–102.
[50] M.A. Amin, S.S. Abd El-Rehim, E.E.F. El-Sherbini, R.S. Bayyomi, The inhibition of low carbon steel corrosion in hydrochloric acid solutions by succinic acid—part I: weight loss, polarization, EIS, PZC, EDX and SEM studies, Electrochim. Acta 52 (2007) 3588–3600.
[51] M.M. Saleh, Inhibition of mild steel corrosion by hexadecylpyridinium bromide in 0.5 M H_2SO_4, Mater. Chem. Phys. 98 (2006) 83–89.
[52] L. Tang, X. Li, L. Li, The effect of 1-(2-pyridylazo)-2-naphthol on the corrosion of cold rolled steel in acid media: Part 2: inhibitive action in 0.5 M sulfuric acid, Mater. Chem. Phys. 97 (2006) 301–307.
[53] S.S.A. Rehim, O.A. Hazzazi, M.A. Amin, K.F. Khaled, On the corrosion inhibition of low carbon steel in concentrated sulfuric acid solutions. Part I: chemical and electrochemical (AC and DC) studies, Corros. Sci. 50 (2008) 2258–2271.
[54] R. Solmaz, E. Altunbaş, G. Kardaş, Adsorption and corrosion inhibition effect of 2-((5-mercapto-1,3,4-thiadiazol-2-ylimino)methyl)phenol Schiff base on mild steel, Mater. Chem. 125 (2011) 796–801.
[55] A.W. Roszakat, D.F. Weaver, 5,5-Diphenyl-2-thiohydantoin, Acta Crystallogr. C54 (1998) 1168–1170.
[56] V. Deval, A. Kumar, V. Gupta, A. Sharma, A. Gupta, Spectrochim. Acta A Mol. Biomol. Spectrosc. 132 (2014) 15–26.
[57] K.B. Wiberg, Y. Wang, A comparison of some properties of CO and CS bonds, Arkivoc (v) 2011, pp. 45–56.
[58] D. Daoud, T. Douadi, S. Issaadi, S. Chafaa, Adsorption and corrosion inhibition of new synthesized thiophene Schiff base on mild steel X52 in HCl and H_2SO_4 solutions, Corros. Sci. 79 (2014) 50–58.
[59] L. Guo, S. Zhu, S. Zhang, Q. He, W. Li, Theoretical studies of three triazole derivatives as corrosion inhibitors for mild steel in acidic medium, Corros. Sci. 87 (2014) 366–375.
[60] X. Li, et al., Corros. Sci. 87 (2014) 27–39.
[61] Z. Cao, Y. Tang, H. Cang, J. Xu, G. Lu, W. Jing, Novel benzimidazole derivatives as corrosion inhibitors of mild steel in the acidic media. Part II: theoretical studies, Corros. Sci. 83 (2014) 292–298.
[62] S. Martinez, Inhibitory mechanism of mimosa tannin using molecular modeling and substitutional adsorption isotherms, Mater. Chem. Phys. 77 (2002) 97–102.
[63] A.Y. Musa, R.T.T. Jalgham, A.B. Mohamad, Molecular dynamic and quantum chemical calculations for phthalazine derivatives as corrosion inhibitors of mild steel in 1 M HCl, Corros. Sci. 56 (2012) 176–183.
[64] I. Ahamad, R. Prasad, M.A. Quraishi, Thermodynamic, electrochemical and quantum chemical investigation of some Schiff bases as corrosion inhibitors for mild steel in hydrochloric acid solutions, Corros. Sci. 52 (2010) 933–942.
[65] D. Ben Hmamou, M.R. Aouad, R. Salghi, A. Zarrouk, M. Assouag, O. Benali, M. Messali, H. Zarrok, B. Hammouti, Inhibition of C38 steel corrosion in hydrochloric acid solution by 4,5-diphenyl-1H-imidazole-2-thiol: gravimetric and temperature effects treatments, J. Chem. Pharm. Res. 4 (2012) 3498–3504.
[66] F. Bentiss, M. Traisnel, L. Gengembre, M. Lagrenee, Inhibition of acidic corrosion of mild steel by 3,5-diphenyl-4H-1,2,4-triazole, Appl. Surf. Sci. 161 (2000) 194–202.